0273-2289/96/6101-02—0001$08.00

Unusual Kinetic Properties of Anionic Tobacco Peroxidase Related to the Mechanism of Oxidation of Indole-3-Acetic Acid

I. G. GAZARIAN,*[1] G. A. ASHBY,[2]
R. N. F. THORNELEY,[2] AND L. M. LAGRIMINI[3]

[1]Department of Chemical Enzymology, Chemical Faculty, Moscow State University, Moscow, 119899 GSP, Russia; [2]Nitrogen Fixation Laboratory, AFRC Institute of Plant Science Research, University of Sussex, Brighton, UK; and [3]Department of Horticulture and Crop Science, Ohio State University, Columbus, OH

ABSTRACT

Anionic tobacco peroxidase (TOP) (mol wt 36 kDa, pI 3.5) was purified from transgenic tobacco plants with the yield of 60 mg/1 kg leaves. The enzyme exhibits unusual properties, i.e., Compound I is less reactive than Compound II. The enzyme was investigated in oxidation of indole-3-acetic acid (IAA) oxidation by oxygen in the air. The aerobic steady-state spectral studies reveal that Compound II is the key intermediate of the reaction mechanism. This was confirmed in the anaerobic stopped-flow experiments. No reaction between the enzyme and IAA is observed under anaerobic conditions. The data obtained are interpreted in terms of a ternary complex formation (ferric enzyme–IAA–oxygen) at the initiation step resulting in production of IAA radicals. The latter interacts with the ferric enzyme and oxygen producing Compound II. The oxidative cycle involves the ferric enzyme and Compound II, and is independent from the peroxidative one.

Index Entries: Compound I, Compound II, oxidative cycle; reaction mechanism; ternary complex; hydrogen peroxide; peroxidative cycle.

*Author to whom all correspondence and reprint requests should be addressed.

Abbreviations: TOP, tobacco anionic peroxidase; HRP, horseradish peroxidase; E, ferric enzyme, native form of peroxidase with Fe (III); ferrous enzyme, reduced Fe (II) state of native peroxidase; Compound I, two-electron oxidized form of ferric peroxidase, the so-called oxyferryl-heme; Compound II, one-electron oxidized form of the ferric enzyme; Compound III, four-electron oxidized state of ferric enzyme; IAA, indole-3-acetic acid (I); $IAA^{\cdot+}$, indole-3-acetate cation-radical (II); $IAA^{\cdot}$, indolyl radical (III); $In\text{-}CH_2^{\cdot}$, indole-3-methyl (skatole) radical (IV); $In\text{-}CH_2O_2^{\cdot}$, skatole peroxyl radical; $In\text{-}CH_2OOH$, skatole hydroperoxide; $In\text{-}CH_2O$, indole-3-epoxide (V); 3-methylene-indolenine (VI).

INTRODUCTION

Elucidation of structure–function relationships for the heme-containing plant peroxidases (EC 1.11.1.7) is closely related to isolation and biochemical description of novel enzymes with the known primary structures. However, further success depends on the amount of enzyme available for detailed studies, including crystallography, NMR, Raman spectroscopy, rapid kinetics, and so on. Thus, the superproduction of peroxidase is necessary for its complete characterization.

Cloning (*1*) and expression (*2*) of the anionic tobacco peroxidase (TOP) gene in transgenic plants lead to the superproduction of the wild-type enzyme and cause the plant wilting that could indicate the involvement of tobacco peroxidase in oxidation of indole-3-acetic acid (IAA), which is a powerful plant hormone responsible for cell growth and elongation.

The oxidative decarboxylation of IAA catalyzed by plant peroxidases is considered to be of great physiological importance. Previous aerobic steady-state and transient kinetic studies of IAA oxidation (*3–6*) were performed using mainly horseradish peroxidase (HRP), and two pathways of IAA oxidation were proposed (*7*). The conventional peroxidative cycle (1)–(3) operates at a high enzyme-to-IAA ratios.

$$\text{Native enzyme} + \text{ROOH} \rightarrow \text{Compound I} + \text{ROH} \quad (1)$$

$$\text{Compound I} + \text{IAA} \rightarrow \text{Compound II} + IAA^{\cdot+} \quad (2)$$

$$\text{Compound II} + \text{IAA} + H^+ \rightarrow \text{Native enzyme} + IAA^{\cdot+}\ H_2O \quad (3)$$

The ferrous enzyme/Compound III shuttle (4)–(6) operates at the low [E]/[IAA] ratios:

$$\text{Native enzyme} + \text{IAA} \rightarrow \text{Ferrous enzyme} + IAA^{\cdot+} \quad (4)$$

$$\text{Ferrous enzyme} + O_2 \rightarrow \text{Compound III} \quad (5)$$

$$\text{Compound III} + \text{IAA} \rightarrow \text{Ferrous enzyme} + \text{P} + CO_2 + H_2O \quad (6)$$

where P is indole-3-aldehyde.

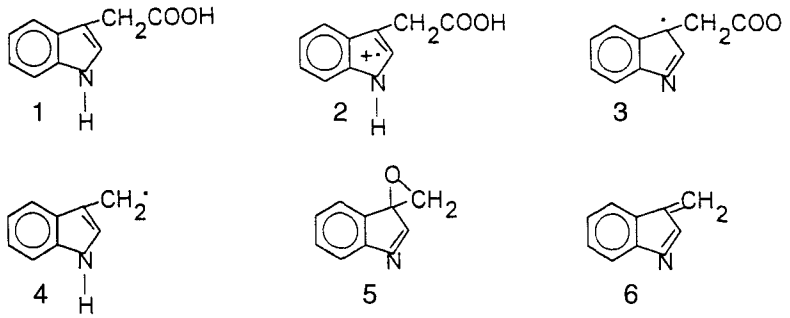

Schemes 1–6

Scheme (1)-(3) suggests the presence of radical species that could lead to an organic hydroperoxide (probably skatole peroxide). Scheme (4)–(6) is widely used (*8*) though the initiation and direct reduction of ferric enzyme to ferrous by IAA have not been demonstrated experimentally. Thus, there is still no consensus about the mechanism of oxidation of IAA catalyzed by plant peroxidases.

The present article describes unusual kinetic features of the newly isolated peroxidase with respect to hydrogen peroxide, and results of the anaerobic transient and aerobic steady-state kinetic study of oxidation of IAA. The results obtained suggest that IAA oxidation by oxygen catalyzed by TOP occurs via the initial formation of the ternary complex ferric enzyme–IAA–oxygen. Compound II is shown to be a key intermediate of the oxidative cycle.

MATERIALS AND METHODS

Enzyme Purification

TOP was purified from transgenic *Nicotiana sylvestris* plants as follows: 1 kg of leaves was collected just before flowering, homogenized in 2 L of 0.1*M* Tris-HCl buffer, pH 6.0, filtered and centrifuged (10,000 rpm, 20 min). The juice obtained (3.5 L) was treated by DEAE-cellulose to remove the pigment, then diluted 10 times, and applied on a DEAE-cellulose column equilibrated with 0.01*M* Tris-HCl buffer, pH 6.0. The enzyme was eluted with 0.1–0.15*M* Tris-HCl buffer, pH 6.0, and then applied on a Sephacryl S-200 column (5 × 100 cm) in 0.01*M* Tris-HCl, pH 6.0. The active fractions were collected, concentrated (up to 10 mg/mL), sterilized by filtration, and stored at 4°C. The homogeneous preparation obtained (60 mg) had a mol wt of 36 kDa and pI 3.5, as was estimated earlier for the wild-type enzyme (*1,9*). The RZ value was in the range 3.4–3.8. The concentration of TOP was determined spectrophotometrically at 403 nm using the molar absorptivity of 108,000M^{-1}/cm.

Oxygen Uptake

Studies were carried out using an oxygen electrode fitted to a plastic chamber (Rank Brothers). Kinetic measurements were performed in the IAA concentration range 0.1–6 m*M* in 0.1 Na-citrate buffer, pH 4.6, 0.1*M* Na-acetate buffer, pH 5.0, and 10 m*M* K-phosphate buffer, pH 6.5 at 22°C using 0.08, 0.1, and 0.25 μM TOP, respectively. The standard deviation in the rate of oxygen uptake determined in three measurements was 5%. The values of K_m and V_m were obtained from double reciprocal plots, and the turnover number was calculated as $V_m/[E]$ where [E] is the enzyme concentration. The effect of hydrogen peroxide in the concentration range 10–300 μM was studied with 0.2 m*M* IAA and 0.05 μM TOP in 50 m*M* Na-citrate buffer, pH 4.5.

Steady-State Spectral Studies

Measurements were performed at 22°C on a Shimadzu UV 160U spectrophotometer. Spectral changes were recorded immediately after addition of hydrogen peroxide (3-s delay). Compound III was preformed adding hydrogen peroxide in 1000-fold excess over the enzyme in 0.1*M* Na-acetate buffer, pH 5.0, and incubating the mixture for 1 min. The spectral changes were recorded immediately after addition of IAA aliquot.

Transient Kinetic Studies

Determination of the rate constant for the interaction of TOP with hydrogen peroxide was performed using a High-Tech SF-61 rapid-scan stopped-flow instrument operated in a single-wavelength regime at 402 nm in 50 m*M* Tris-HCl buffer, pH 8.0, 23°C. TOP was shot against increasing concentrations of H_2O_2, and the kinetic curves obtained were fitted to the equation $A = A_0 exp - kt$ where A is absorbance, k is the apparent first-order rate constant, and t is time. The values of k were plotted against $[H_2O_2]$, and the second-order rate constant was calculated from the slope of a linear plot. The following final concentrations were used: TOP 1 μM, and hydrogen peroxide 2.5, 5, 7.5, 10, and 15 μM.

Anaerobic transient studies of the oxidation of IAA were performed using the same device equipped with a diode array detector (supplied with a 360-nm filter to reduce radiolysis) and a tungsten lamp. The stopped-flow apparatus was installed in an anaerobic glove box operated under N_2 with <1 ppm of O_2. The TOP stock solution and buffers (50 m*M* Na-citrate, pH 4.5, and 50 m*M* K-phosphate, pH 7.0) were deoxygenated for 40 min before placing into the glove box. The air-saturated buffer was placed into the anaerobic box in a hermetically closed vessel. The stock solution of IAA (Sigma) (50 m*M*) was prepared in the dark under anaerobic conditions in 0.1*M* Tris-HCl buffer, pH 8.7, and then anaerobically diluted five times with the corresponding buffer.

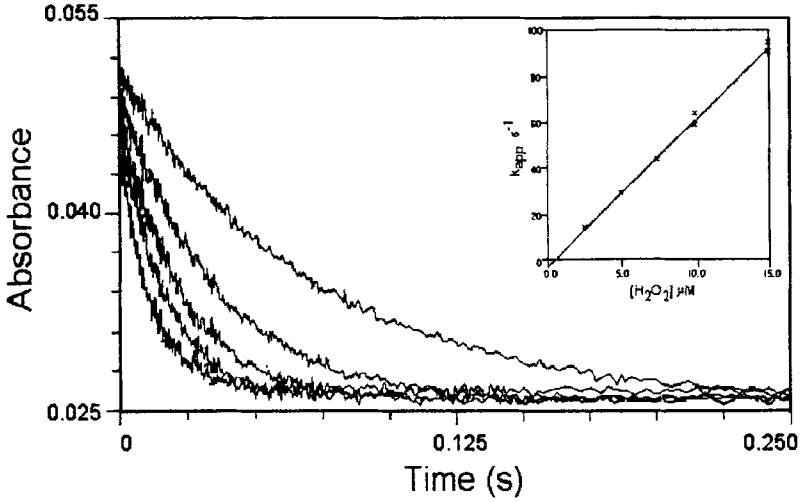

Fig. 1. Determination of the rate constant for the interaction of TOP with hydrogen peroxide. Absorbance changes at 403 nm with $[H_2O_2]$ = 2.5, 5.0, 7.5, 10, and 20 μM and 2 μM TOP in 50 mM Tris-HCl buffer, pH 8.0. Inset—dependence of k on $[H_2O_2]$.

RESULTS AND DISCUSSION

TOP Interaction with Hydrogen Peroxide

The transient kinetics of the interaction of TOP with increasing concentrations of hydrogen peroxide is in Fig. 1. The apparent first-order rate constants were proportional to the concentration of H_2O_2 (Fig. 1B). Thus, the second-order rate constant for the interaction between TOP and H_2O_2 = $6.3 \times 10^6 M^{-1}/s$, and it is three times lower than that for HRP C (*5*).

The steady-state spectral study of the interaction of TOP with hydrogen peroxide (Fig. 2) demonstrated unusual properties of the enzyme. Very stable Compound I was formed in 3- to 300-fold excess of hydrogen peroxide. It has a characteristic shoulder at 350 nm in the Soret band, and peaks at 554 and 655 nm (Fig. 2A, curve 2). The spectrum is unchanged within 15–20 min. This is in contrast to HRP, which reacts with an equimolar amount of hydrogen peroxide forming a mixture of Compounds I and II independent of the enzyme concentration (*10*). Relatively pure Compound I of HRP could be obtained only if the enzyme is pretreated with hydrogen peroxide (*11*). An attempt to obtain a spectrum of the TOP Compound II at pH 4.5–5.0 was unsuccessful. Compound I converted directly into Compound III (Fig. 2A, curve 3) in a large excess of the peroxide.

It was possible to detect the spectrum of Compound II at pH 7.5 and a 30- to 50-fold excess of H_2O_2 with the characteristic peaks at 527 and 557 nm (Fig. 2B). However, the broadness of the Soret band suggested the presence of Compound I.

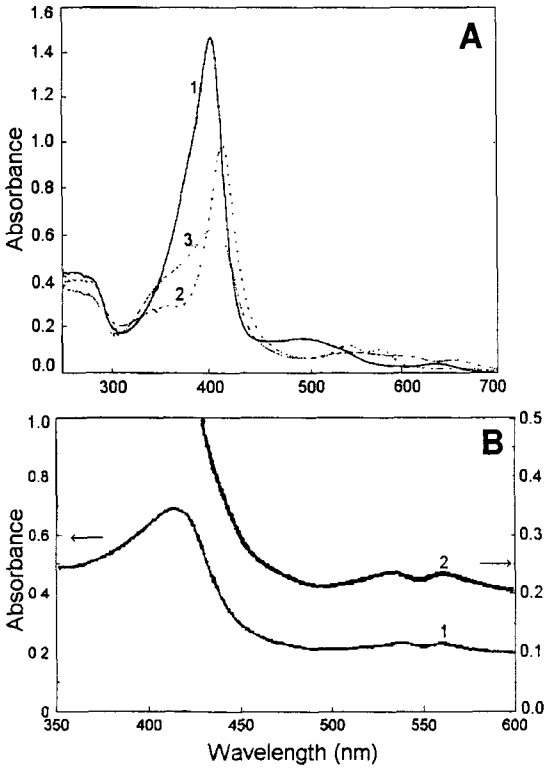

Fig. 2. Spectra of TOP compounds. (**A**) Native enzyme (1), Compound I (2) and III (3) obtained by addition of 50- and 1000-fold excess of hydrogen peroxide, respectively, in 50 m*M* Na-citrate buffer, pH 4.5. (**B**) Appearance of Compound II after 2-min incubation of 10 μM TOP with 300 μM hydrogen peroxide in 0.1*M* K-phosphate buffer, pH 7.5. Absorbance range 1.0 (1) and 0.5 (2).

Thus, newly isolated TOP exhibits very interesting kinetic properties. In particular, its Compound I is very stable and less active than Compound II. This is in contrast to other plant peroxidases, including commercial HRP C. At neutral pH, the reactivity of Compound II drops and becomes close to that of Compound I, indicating that pH could significantly affect the rates of TOP-catalyzed reactions.

Catalytic Properties of TOP in Oxidation of IAA

In the course of TOP-catalyzed oxidation of IAA by oxygen in the air, the native enzyme was a dominant steady-state form detected. However, at neutral pH (>6.0), it was possible to detect Compound II just after mixing of the reagents (Fig. 3A), though it converted back into the native form in a matter of a minute. Kinetic parameters of the IAA aerobic oxidation catalyzed by TOP obtained from oxygen uptake measurements (Table 1) demonstrate the dependence of the maximal rates on pH, although changes in K_m are insignificant. One can ascribe this to the pH dependence of the reactivity of Compound II, if this form is responsible for the oxidation.

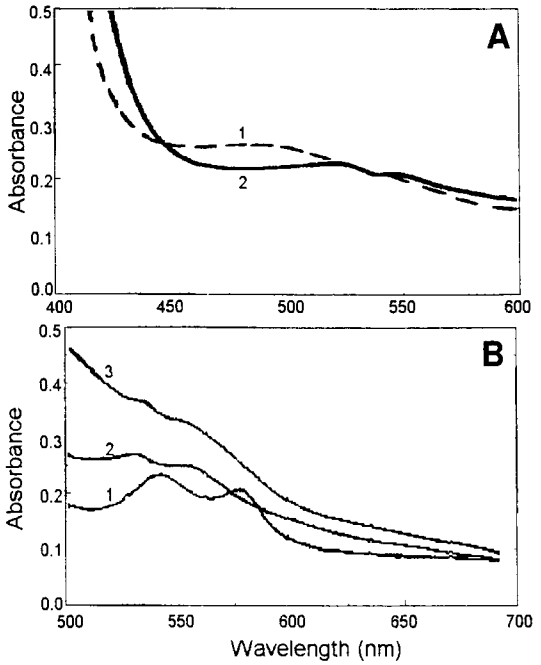

Fig. 3. Steady-state spectra in the course of IAA oxidation (**A**) Absorbance changes recorded just after 10 μM TOP addition (3-delay) (1) to 0.5 mM IAA solution in 0.1M Tris-HCl buffer, pH 6.0, and 1 min later (2). (**B**) The visible spectra initiated by 1 mM IAA addition to 18 μM of preformed TOP Compound III in 0.1M Na-acetate buffer, pH 5.0. (1) Compound III and (2), (3) Compound II spectra recorded 3 and 30 s, respectively, after IAA addition to Compound III.

Table 1
Kinetic Parameters for IAA Oxidation by Tobacco Peroxidase
($5 \times 10^{-8}M$ Peroxidase, 0.2–2 mM IAA)

Buffer	Na-acetate	Na-citrate	K-phosphate
pH	5.0	4.6	6.5
K_m, mM	0.75 ± 0.05	0.6 ± 0.1	1.2 ± 0.2
Turnover number, s^{-1}	50 ± 3	33 ± 3	7 ± 3

The homogeneous preparation of TOP catalyzed the oxidation of IAA by oxygen in the air without phenols, manganese (II), salts and hydrogen peroxide. However, the latter stimulated the oxygen uptake (Table 2). Hydrogen peroxide affected the initial rate of oxygen consumption and completely eliminated the lag period observed on kinetic curves in the absence of hydrogen peroxide (not shown). The acceleration by hydrogen peroxide was associated with the appearance of Compound II in the steady-state spectral experiments (not shown). Compound II was observed as long as hydrogen peroxide and oxygen were present in the system. Thus,

Table 2
Effect of Hydrogen Peroxide on IAA Oxidation by Tobacco Peroxidase
($5 \times 10^{-8}M$ Peroxidase, 0.2 m*M* IAA, Na-citrate Buffer, pH 4.5)

Hydrogen peroxide concentration, μM	0	10	20	50	100	300
Reaction rate, μM O_2/min	66	70	100	110	144	140
Reaction rate, %	100	106	152	167	202	201

the elimination of lag period and acceleration of IAA oxidation by hydrogen peroxide were owing to generation of Compound II via the peroxidative cycle. Moreover, an addition of IAA to the preformed TOP Compound III gave also the spectrum of Compound II (Fig. 3B), whereas in the case of HRP, the addition of IAA only accelerated the decomposition of Compound III and the formation of so-called Compound P-670 (*8*). Taking into account all observations, it can be assumed that Compound II could be a key intermediate responsible for IAA oxidation.

The Mechanism of IAA Oxidation by Tobacco Peroxidase

The data obtained previously on IAA oxidation catalyzed by HRP C (*4,5*), HRP A (*5*), and turnip peroxidase (*4*) indicated also participation of Compound II. However, the formation of Compound II in the course of IAA oxidation was usually interpreted as a main feature indicative of the peroxidative cycle (1)–(3) (*7*). To throw some light on the problem, we used anaerobic transient kinetic technique to study the mechanism of IAA oxidation.

The data obtained (Figs. 4 and 5) made us reconsider the widely accepted mechanistic scheme (4)–(6) involving the ferrous enzyme (*8,9*). First, it has been shown that IAA is unable to reduce TOP directly under anaerobic conditions (Fig. 4A), and all spectral changes are observed only in a ternary system, including IAA, oxygen, and the enzyme (Fig. 4B and C). This allows interpretation of the reaction mechanism in terms of a ternary complex (*7*), which could be formed by the sequential binding of both substrates followed by the final formation of the IAA cation radical:

$$\begin{aligned} &E + IAA \rightarrow E\text{-}IAA + O_2 \rightarrow [E\text{-}IAA - O_2] \leftrightarrow \\ &[E\text{-}IAA^{\cdot+} - O_2^{\cdot-}] \rightarrow E + IAA^{\cdot+} + O_2^{\cdot-} \end{aligned} \quad (7)$$

The involvement of the IAA cation radical accounts for the mechanistic differences in acidic (Fig. 4B) and neutral meia (Fig. 4C). The reactivity of $IAA^{\cdot+}$ *is pH-dependent* (*12*). It undergoes decarboxylation (*8*) with a first-order rate constant of 18,000 s^{-1}, whereas at neutral pH, it converts rapidly into the indolyl radical (*9*) via proton release (pK_A = 5.1). the indolyl radical presumably decarboxylates via binary interactions, because its decarboxylation rate constant is < 100 s^{-1} (*12*).

$$IAA^{\cdot+} \rightarrow In\text{-}CH_2^{\cdot} + CO_2 \quad (8)$$

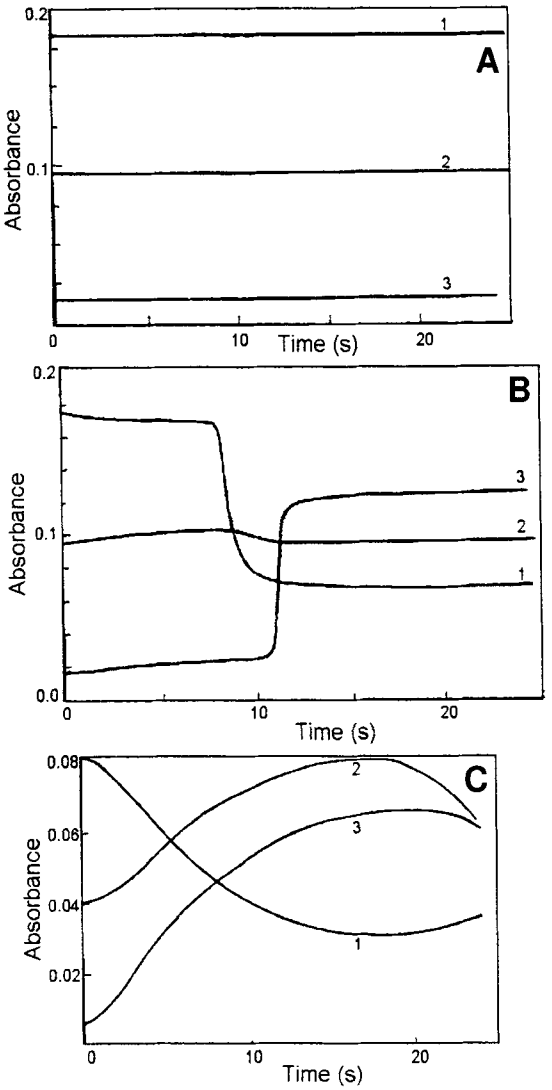

Fig. 4. Spectral changes at 403 (1), 416 (2), and 433 nm (3) in the course of IAA interaction with TOP. (**A**) 1.8 μM TOP interaction with 5 mM IAA under strict anaerobic conditions in 50 mM Na-citrate buffer, pH 4.5. (**B**) The same experiment performed in the presence of 50 μM oxygen (premixed with IAA). (**C**) 1.6 μM *TOP shut against 5 mM* IAA pre-mixed with 50 μM oxygen in 50 mM K-phosphate buffer, pH 7.0. The initial absorbances at 403, 416, and 433 nm were 0.175, 0.100 and 0.030.

$$IAA^{\cdot +} \rightarrow IAA^{\cdot} + H^{+} \quad (9)$$

Skatole radicals participate in a number of non-enzymatic processes in the presence of oxygen leading to skatole peroxyl (*10*), skatole hydroperoxide (*11*), and indolyl radicals. These reactions interfere and complicate the enzymatic process, launching the peroxidative cycle (1)–(3) with the organic hydroperoxide (skatole peroxide).

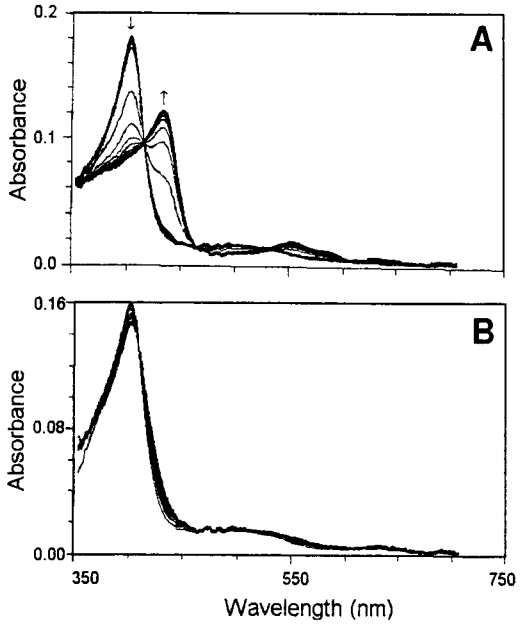

Fig. 5. Rapid scans of TOP interaction with IAA premixed with oxygen in 50 m*M* Na-citrate buffer, pH 4.5 (**A**) and 50 m*M* K-phosphate buffer, pH 7.0 (**B**) corresponding to the single-wavelength experiments in Fig. 4B and C, respectively. Ninety-six scans were performed in the range from 1.2 ms to 24s. The first scan from each series of eight is presented.

$$IV + O_2 \rightarrow In\text{-}CH_2O_2^{\cdot} \quad (10)$$

$$In\text{-}CH_2O_2^{\cdot} + IAA \rightarrow In\text{-}CH_2OOH + IAA^{\cdot} \quad (11)$$

However, it was also suggested that nonenzymatic decomposition of skatole hydroperoxide is more probable (*7*).

Rapid scans at low pH (Fig. 5A) showed nearly no spectral changes during the phase corresponding to oxygen consumption. The kinetic traces recorded at 416 nm (the isosbestic point for ferric and ferrous TOP) (Fig. 4B) indicate the presence of Compound II. The appearance of the ferrous enzyme after all oxygen is consumed can be explained by reduction of the ferric enzyme into the ferrous one by skatole radicals (*12*):

$$TOP(Fe^{3+}) + In\text{-}CH_2^{\cdot} \rightarrow TOP(Fe^{2+}) + In\text{-}CH_2^{+} \quad (12)$$

The redox potential of the ferric/ferrous enzyme pair depends on pH (*13*). At pH 7.0, it equals −275 mV. It is much lower at acidic pH (−155 and −105 mV at pH 5.0 and 4.0, respectively), and that is why the ferrous enzyme is mainly observed in acidic media. The skatole cation $In\text{-}CH_2^{+}$ converts into 3-methylene-indolenine via proton release, and the latter polymerizes easily giving rise to a large amount of nonidentified polymeric products (*6*).

Figure 5B shows that at neutral pH, the only form of enzyme detected is Compound II, confirming its key role in the oxidation of IAA. The ferric

enzyme is converted directly into Compound II with a well-defined isosbestic point at 408 nm. Therefore, the oxidative cycle includes ferric enzyme and Compound II:

$$E + IAA^{\cdot} \rightarrow E\text{-}IAA^{\cdot} \quad (13)$$

$$E\text{-}IAA^{\cdot} + O_2 \rightarrow E(OH^{\cdot}) + In\text{-}CH_2O + CO_2 \quad (14)$$

Compound II

$$E(OH^{\cdot}) + IAA \rightarrow E\text{-}IAA^{\cdot} + H_2O \quad (15)$$

The formation of indole-3-epoxide was proposed by Ricard and Job more than 20 years ago to account for the results of the aerobic stopped-flow studies of the oxidation of IAA by HRP C and turnip peroxidases at low temperatures (*8*).

The oxidative cycle, including initiation (*7*) and the main cycle (14)–(15), is independent from the peroxidative one. The latter provides an additional route to Compound II promoting the IAA oxidation. Actually, the accelerating effect of hydrogen peroxide was earlier reported for the anionic isozyme HRP A (*5*). In the case of cationic peroxidases, HRP C and turnip enzyme (*4*), hydrogen peroxide inhibits oxygen consumption. Compound III was reported as an intermediate (*4,5,7,8*), and its direct two-electron reduction by IAA (*4*) gives an additional route to Compound II.

The absence of Compound III in the course of IAA oxidation as well as unusual kinetic properties of TOP in the reaction with hydrogen peroxide can be ascribed to its primary structure. All plant peroxidases are characterized by highly constant sequences involved in coordination of heme. However, they exhibit a variety of sequences controlling the accessibility of the active center, the so-called entrance to the heme-binding pocket. The comparison of these sequences for TOP and HRP shows the presence of the negatively charged group, viz. Glu-141, in TOP (*1*) which corresponds to Phe-143 in HRP C (*14*):

HRP 138 Leu-Pro-Ala-Pro-Phe-Phe 143
TOP 136 Ile-Pro-Ser-Pro-Phe-**Glu** 141

The glutamate residue seems to affect the stability of Compound I and the enzyme reactivity toward hydrogen peroxide and superoxide radicals. We associate the unusual kinetic properties of TOP with the negative charge at the entrance of the heme-binding pocket. This affects the substrate specificity of TOP, which is currently under investigation.

CONCLUSIONS

The catalytic properties of TOP are different compared to those of HRP C, and this allows new insight into the problem of IAA oxidation by plant peroxidases investigated since 1955. The data on anaerobic transient

kinetics for the oxidation of IAA oxidation obtained in this study demonstrate that the reaction proceeds via a ternary complex enzyme-IAA-oxygen responsible for radical generation. The initiation step is followed by the oxidative cycle where Compound II and the ferric enzyme complex with indolyl radical play the major role. Plant peroxidases could be considered as oxygenases in the oxidation of IAA by oxygen, and the reaction itself might exemplify the main physiological function of these heme-containing enzymes.

REFERENCES

1. Lagrimini, L. M., Burkhart, W., Moyer, M., and Rothstein, S. (1987), *Proc. Natl. Acad. Sci. USA* **84,** 7542–7546.
2. Lagrimini, L. M., Bradford, S., and Rothstein, S. (1990), *Plant Cell* **2,** 7–18.
3. Hinman, R. L. and Lang, J. (1965), *Biochemistry* **4,** 144–158.
4. Ricard, J. and Job, D. (1974), *Eur. J. Biochem.* **44,** 359–374.
5. Nakajima, R. and Yamazaki, I. (1979), *J. Biol. Chem.* **254,** 872–878.
6. Kobayashi, S., Sugioka, K., Nakano, H., Nakano, M., and Tero-Kubota, S. (1984), *Biochemistry* **23,** 4589–4597.
7. Smith, A. M., Morrison, W. L., and Milham, P. J. (1982), *Biochemistry* **21,** 4414–4419.
8. Metodiewa, D., Pires de Melo, M., Escobar, J. A., Cilento, G., and Dunford, H. B. (1992), *Arch. Biochem. Biophys.* **296,** 27–33.
9. Egorov, A. M., Reshetnikova, I. A., Fechina, V. A., and Gazaryan, I. G. (1994), *Ann. NY Acad. Sci.* **750,** 469–472.
10. Blumberg, W. E., Peisach, J., Wittenberg, B. A., and Wittenberg, J. B. (1968), *J. Biol. Chem.* **243,** 1854–1862.
11. Chance, B. (1952), *Arch. Biochem. Biophys.* **41,** 416–422.
12. Candeias, L. P., Folkes, L. K., Dennis, F. D., Patel, K. B., Everett, S. A., Stratford, M. R. L., and Wardmann, P. (1994), *J. Phys. Chem.* **98,** 10,131–10,137.
13. Harbury, H. A. (1957), *J. Biol. Chem.* **255,** 1009–1024.
14. Welinder, K. G. (1979), *Eur. J. Biochem.* **96,** 483–502.